Letter

Large deviations of a tracer position in the dense and the dilute limits of single-file diffusion

Jagannath Rana* and Tridib Sadhu

Department of Theoretical Physics, Tata Institute of Fundamental Research, 1 Homi Bhabha Road, Mumbai 400005, India

(Received 3 March 2022; revised 15 November 2022; accepted 4 January 2023; published 17 January 2023)

We apply the macroscopic fluctuation theory to analyze the long-time statistics of the position of a tracer in the dense and the dilute limits of diffusive single-file systems. Our explicit results are about the corresponding large deviation functions for an initial step density profile with the fluctuating (annealed) and the fixed (quenched) initial conditions. These hydrodynamic results are applicable for a general single-file system and they agree with recent exact results obtained by microscopic solutions for specific model systems.

DOI: 10.1103/PhysRevE.107.L012101

Introduction. A one-dimensional interacting many-particle system with a restriction that particles cannot bypass each other is called a single-file system. Due to the single-file constraint, a large displacement of an individual particle needs to push surrounding particles in the same direction (see Fig. 1). This caging effect leads to nontrivial transport properties. Most notably, a tracer particle follows subdiffusion with a diffusivity that is sensitive to the initial condition even at large times [1–3]. In general, for large times, the subdiffusion corresponds to the fractional Brownian motion with Hurst exponent $H = 1/4$ [1,3,4].

The single-file system was introduced more than 60 years ago as a model to describe ion transport through cell membranes [5]. Since then a wide variety of physical, chemical, and biological processes have been described using single file motion: Molecular diffusion inside a porous zeolite medium [6,7], water transport inside carbon nanotube [8], sliding of large protein molecules inside DNA [9], and transport of ions through super-ionic conductors [10] are just a few such examples.

The subdiffusive nature was first theoretically shown by Harris [11] for Brownian point particles with hard-core repulsion and subsequently demonstrated in experimental systems [8,12–15]. There have been numerous attempts [16–19] to extract the statistics of tracer position in general single-file systems with arbitrary interaction. Most general results are available for the mean and the variance of the tracer position. Calculation of all the cumulants, equivalently the cumulant generating function (CGF) of tracer position in general single-file systems is still a challenging open problem.

A remarkable exact result for the tracer-CGF is in the single-file system of symmetric exclusion process where the result was derived by a solution of the microscopic dynamics for a fluctuating (annealed) initial state [20,21]. There are no analogous results available for general single-file systems. For a fixed (quenched) initial state of the symmetric exclusion process, there are exact results for half-filling [3] and for the high-density limit, [22]. The low-density limit of the symmetric exclusion process corresponds to the hard-core Brownian particles, which was exactly solved [2,16].

In this Letter, we present a unified approach for several of these earlier model-specific results [20,22,23] and generalize them for a larger class of systems. This approach is based on a perturbation solution of a fluctuating hydrodynamic theory [2] in the low and high-density limit. Our main results are about an exact expression for the CGF in a *generic* diffusive single-file system in the two limits for both annealed and quenched initial settings.

The fluctuating hydrodynamic approach in [2] is an application of the macroscopic fluctuation theory (MFT) [24–28] that was developed two decades ago and extends the Onsager-Machlup theory [29] for far-from-equilibrium states. The theory is defined in a macroscopic scale where all microscopic details are embedded in a finite number of transport coefficients. For the diffusive single-file systems that we consider, the mobility $\sigma(\rho)$ and the diffusivity $D(\rho)$ are the relevant transport coefficients [2,28] which are functions of the locally conserved macroscopic density of particles $\rho(x,t)$. In this approach, the problem of calculating the CGF of tracer position in a single-file reduces to a variational problem, which is hard to solve in general [2]. Recently, there has been remarkable progress in exact solutions [21,30–32] of the variational problem for related observables. These solutions based on integrability techniques are a tour de force, but specific to the models and the observables concerned. For generic transport coefficients, a solution of the variational problem still remains intractable except for the specific boundary condition related to the CGF of currents [33].

We show that for the tracer diffusion the variational problem can be systematically approached using a perturbation expansion in density. To the leading order, we get the CGF in the dilute and the dense limits for a generic single-file diffusion. For the special case of the symmetric exclusion process, our results agree with the expression of CGF obtained by microscopic solutions [20,22,23].

Besides generality, the hydrodynamic approach gives additional information about how the surrounding density profile is correlated with the tracer displacement, which is recently reported using exact microscopic calculations [21,34].

*jagannath.rana@tifr.res.in

FIG. 1. A realization of a single-file system where particles confined in a narrow channel are constrained such that no particle can cross each other. The red particle denotes a tracer in the bath of identical other particles (blue).

Hydrodynamic formulation. In a coarse-grained description, time evolution of density field $\rho(x,t)$ in a single-file diffusion is given [2,28] by the fluctuating hydrodynamics equation

$$\partial_t \rho = -\partial_x j \quad \text{with } j = -D(\rho)\partial_x \rho + \sqrt{\sigma(\rho)}\,\eta, \tag{1}$$

where $\eta(x,t)$ is a zero-mean Gaussian noise with covariance $\langle \eta(x,t)\eta(x',t')\rangle = \delta(x-x')\delta(t-t')$. Here $\rho(x,t)$ is the dimensionless occupied-volume-fraction. A local equilibrium condition relates the two transport coefficients to the free energy density $f(\rho)$ by a fluctuation-dissipation relation $2D(\rho) = \sigma(\rho) f''(\rho)$ [35]. Displacement of a tracer X_t at time t is related to the density field by the single-file constraint [2]

$$\int_0^{X_t} dx\, \rho(x,t) = \int_0^{\infty} dx\, (\rho(x,t) - \rho(x,0)), \tag{2}$$

where the tracer is assumed to be initially at the origin. This relation (2) gives the tracer position X_t as a functional of the history of density $\rho(x,t)$. Different noise realizations of $\eta(x,t)$ in Eq. (1) generate different histories for $\rho(x,t)$, which in turn results in different displacements of the tracer. Probability weight for a history of $\rho(x,t)$ is given by an action, which comes straightforwardly following the Martin-Siggia-Rose-Janssen-de-Dominicis (MSRJD) formalism [2,35,36] for Eq. (1). The additional source of stochasticity comes from initial state. Considering probability of density fluctuations in the initial state $P(\rho(x,0)) \sim e^{-F(\rho(x,0))}$ (the $\sim$ denotes leading dependence in the hydrodynamic scale), the generating function $\langle e^{\lambda X_T}\rangle$ of the tracer position at time T can be expressed as a pathintegral [2]

$$\langle e^{\lambda X_T}\rangle = \int \mathcal{D}[\rho,\hat{\rho}]\, e^{-S_T[\hat{\rho},\rho]}, \tag{3}$$

where $\hat{\rho}(x,t)$ is the MSRJD response field and the action

$$S_T[\hat{\rho},\rho] = -\lambda X_T[\rho] + F[\rho(x,0)] + \int_0^T dt \int_{-\infty}^{\infty} dx \times \left(\hat{\rho}\,\partial_t \rho - \frac{\sigma(\rho)}{2}(\partial_x \hat{\rho})^2 + D(\rho)(\partial_x \rho)(\partial_x \hat{\rho})\right). \tag{4}$$

For the action to be meaningful we assume that ρ and $\hat{\rho}$ vanish at $x \to \pm\infty$, which does not affect the tracer statistics at finite T.

A rescaling of the spatial coordinate by $\sqrt{T}$ and time by T, shows that S_T is proportional to $\sqrt{T}$. Then for large T, the path integral in (3) is dominated by the path $(\hat{\rho},\rho) \equiv (p,q)$ that minimizes the action and the cumulant generating function $\mu = \ln\langle e^{\lambda X_T}\rangle$ of the tracer for large time T is given by neg ative of the minimal action. A variational calculation gives the least-action path as a solution of [2]

$$\begin{aligned} \partial_t p + D(q)\partial_{xx} p &= -\frac{\sigma'(q)}{2}(\partial_x p)^2 \\ \partial_t q - \partial_x(D(q)\partial_x q) &= -\partial_x(\sigma(q)\partial_x p), \end{aligned} \tag{5}$$

with appropriate boundary conditions that depend on the initial state.

To illustrate an unusual long-time memory effect for the single-file transport, two types of initial states are usually studied [1,2]. For the annealed case the initial state is in equilibrium, with [2,35]

$$F(\rho(x)) = \int_{-\infty}^{\infty} dx \int_{\bar{\rho}(x)}^{\rho(x)} dr\, \frac{2D(r)}{\sigma(r)}(\rho(x) - r), \tag{6}$$

where $\bar{\rho}(x)$ is the mean-density profile of the initial state. In this case, the boundary conditions are on the field $p(x,t)$,

$$\begin{aligned} p(x,0) &= -\lambda \frac{\delta X_T}{\delta q(x,0)} + \frac{\delta F}{\delta q(x,0)}, \\ p(x,T) &= \lambda \frac{\delta X_T}{\delta q(x,T)}. \end{aligned} \tag{7}$$

A quenched setting corresponds to the case where the initial density profile is fixed at the mean-density $\bar{\rho}(x)$ and no fluctuations are allowed. In this case $F(\rho(x,0)) = 0$ and the boundary conditions are

$$q(x,0) = \bar{\rho}(x) \quad \text{and} \quad p(x,T) = \lambda \frac{\delta X_T}{\delta q(x,T)}. \tag{8}$$

The names annealed and quenched are inspired by similar ensembles in disordered systems [37]. In analogy with the partition function in spin glass we define the annealed CGF $\mu_{\mathcal{A}} = \ln\langle e^{\lambda X_T}\rangle_{\text{history+initial}}$ and the quenched CGF $\mu_{\mathcal{Q}} = \langle \ln\langle e^{\lambda X_T}\rangle_{\text{history}}\rangle_{\text{initial}}$ where the initial profile is analogous to disorder. In the latter definition, the logarithm being a slowly varying function compared to $e^{-F(\rho)}$, contribution to $\langle\rangle_{\text{initial}}$ is dominated by the mean-profile $\bar{\rho}(x)$ and this justifies our choice for the fixed initial density in the variational formulation for the quenched case.

For both initial settings, the minimal action reduces to a simple expression [2]

$$S_T[p,q] = -\lambda Y + F(q(x,0)) + \int_0^T dt \int_{-\infty}^{\infty} dx\, \frac{\sigma(q)}{2}(\partial_x p)^2, \tag{9}$$

with $Y \equiv X_T[q]$ for the least action path. A solution of the least-action path (5) with appropriate boundary conditions and the appropriate $F[\rho]$ function gives the CGF $\mu \simeq -S_T[p,q]$ for large T in the corresponding ensemble.

An explicit solution for the least-action path (5) for arbitrary $D(\rho)$ and $\sigma(\rho)$ is not available. A perturbation solution in λ is possible [2] which leads to first few moments of tracer position, but not the CGF. We take an alternative avenue by treating density as a perturbation parameter, which gives the CGF as a series in density. We consider two cases, the dilute and the dense limit, and determine the CGF for general singlefile in both annealed and quenched settings.

Although the hydrodynamic formulation is applicable to an arbitrary initial profile, we consider an example of step density profile $\bar{\rho}(x) = \rho_a \Theta(-x) + \rho_b \Theta(x)$, which has been

frequently studied for tracer diffusion [20,22,23,38]. For $\rho_a \neq \rho_b$, the bulk of the system evolves towards an asymptotic equilibrium effectively biasing the tracer in one direction. For the annealed setting, the two halves of the system are initially in equilibrium at different densities, and they are joined together for $t > 0$.

Dense limit. The density in (1) is the dimensionless occupied-volume-fraction with a maximum value of one. For a simple exclusion process, $\rho(x)dx$ gives the fraction of occupied sites in a hydrodynamic length between x and $x + dx$. In the limit where ρ_a and ρ_b are close to value one, there are very few number of vacant spaces in the single-file. In this limit the transport coefficients $D(\rho) \simeq D(1)$, and $\sigma(\rho) \simeq (\rho - 1)\sigma'(1)$. [Vanishing mobility for $\rho \to 1$ can be understood from the fluctuation-dissipation relation $2D(\rho) = \sigma(\rho)f''(\rho)$, and that in the dense limit leading contribution to the free energy density $f(\rho)$ comes from the positional entropy of voids.]

We consider an expansion for the least-action path, $q = 1 + q_1 + q_2 + \cdots$ and $p = p_0 + p_1 + p_2 + \cdots$, where the subscript denotes the order in $1 - \rho$. To leading nontrivial orders the least-action path in Eq. (5) follows

$$\begin{aligned} D(1)^{-1}\partial_t p_0 + \partial_{xx} p_0 &= -\alpha(\partial_x p_0)^2, \\ D(1)^{-1}\partial_t q_1 - \partial_{xx} q_1 &= -2\alpha\partial_x(q_1\partial_x p_0), \end{aligned} \tag{10}$$

where $\alpha = \sigma'(1)/2D(1)$. We shall see that solution at this order is sufficient for determining the leading term in the CGF.

A canonical transformation [39] $P = e^{\alpha p_0}$ and $Q = q_1 e^{-\alpha p_0}$ reduces the equations (10) to a decoupled diffusion and an antidiffusion equation which are easy to solve, leading to a general solution

$$e^{\alpha p_0(x,t)} = \int_{-\infty}^{\infty} dz\, e^{\alpha\, p_0(z,T)}\, g_{T-t}(z - x), \tag{11a}$$

$$q_1(x,t) = \int_{-\infty}^{\infty} dz\, q_1(z,0)\, e^{-\alpha(p_0(z,0) - p_0(x,t))}\, g_t(z - x), \tag{11b}$$

with the diffusion kernel

$$g_t(x) = \frac{\exp\left(-\frac{x^2}{4D(1)t}\right)}{\sqrt{4\pi D(1)t}}. \tag{12}$$

(a) Quenched case. For the quenched case, perturbation expansion of the boundary condition in Eq. (8) gives $q_1(x,0) = \rho_a\Theta(-x) + \rho_b\Theta(x) - 1$, and $p_0(x,T) = \lambda\Theta(x)$, where we used an expansion $X_T[q] \equiv Y = Y_1 + \cdots$. (Vanishing of Y_0 is understood from the absolute confinement of tracer in the fully packed limit.) Expanding Eq. (2) we get

$$Y_1 = \int_0^{\infty} dx(q_1(x,T) - q_1(x,0)) \tag{13}$$

and with this a perturbation expansion of Eq. (9) gives the leading order term of the CGF

$$\mu_{\mathcal{Q}}(\lambda) \simeq \lambda Y_1 - \frac{\sigma'(1)}{2}\int_{-\infty}^{\infty} dx\, q_1\,(\partial_x p_0)^2, \tag{14}$$

where we used $F[q] = 0$. The expression is further simplified [40] to

$$\begin{aligned} \mu_{\mathcal{Q}}(\lambda) \simeq &-(1-\rho_b)\int_0^{\infty} dx\,(p_0(x,0) - \lambda) \\ &-(1-\rho_a)\int_0^{\infty} dx\, p_0(-x,0), \end{aligned} \tag{15}$$

by using (13), an identity

$$\begin{aligned} (1/2)\sigma'(1)q_1(\partial_x p_0)^2 = &\partial_t(q_1\, p_0) \\ &+ \partial_x[D(1)(q_1\partial_x p_0 - p_0\partial_x q_1) \\ &+ \sigma'(1)q_1 p_0\partial_x p_0] \end{aligned} \tag{16}$$

that comes from Eq. (10), and by using the vanishing q_1 and p_0 at $x \to \pm\infty$. An explicit expression for the CGF in Eq. (15) is then obtained by using the solution for $p_0(x,0)$ in (11a) for the quenched boundary condition, which gives

$$\mu_{\mathcal{Q}}(\lambda) \simeq -\frac{\sqrt{4D(1)T}}{\alpha}\, R_{\mathcal{Q}}(0, \alpha\lambda|1-\rho_a, 1-\rho_b) \tag{17a}$$

in the dense limit, where

$$\begin{aligned} R_{\mathcal{Q}}(y,b|r,s) = &\, r\int_y^{\infty} d\xi\, \ln\left[1 + \frac{e^b - 1}{2}\mathrm{erfc}(\xi)\right] \\ &+ s\int_{-y}^{\infty} d\xi\, \ln\left[1 + \frac{e^{-b} - 1}{2}\mathrm{erfc}(\xi)\right]. \end{aligned} \tag{17b}$$

(b) Annealed case. The boundary condition (7) for $p(x,T)$ is identical to that in the quenched case, therefore the solution for $p_0(x,t)$ from Eq. (11a) is the same in both cases. A straightforward perturbation expansion of the second boundary condition in (7) expresses $q_1(x,0)$ in terms of $p_0(x,0)$,

$$q_1(x,0) = \begin{cases} -(1-\rho_a)e^{\alpha p_0(x,0)}, & \text{for } x \leqslant 0, \\ -(1-\rho_b)e^{\alpha(p_0(x,0) - \lambda)}, & \text{for } x > 0, \end{cases} \tag{18}$$

which is then used in (11b) for an explicit solution for $q_1(x,t)$. Following a similar perturbation analysis of the minimal action in Eq. (9), and using the above boundary condition for $q_1(x,0)$ leads to a simple expression for the leading term of CGF in the dense limit,

$$\begin{aligned} \mu_{\mathcal{A}}(\lambda) \simeq &-\frac{(1-\rho_a)}{\alpha}\int_{-\infty}^{0} dx\,(e^{\alpha p_0(x,0)} - 1) \\ &-\frac{(1-\rho_b)}{\alpha}\int_0^{\infty} dx\,(e^{-\alpha\lambda + \alpha p_0(x,0)} - 1), \end{aligned} \tag{19}$$

which with the solution for $p_0(x,0)$ gives an explicit expression for $\mu_{\mathcal{A}}(\lambda)$ that is almost identical in form to (17a), except the $R_{\mathcal{Q}}$ replaced by $R_{\mathcal{A}}$ where

$$\begin{aligned} R_{\mathcal{A}}(y,b|r,s) = &\, r(e^b - 1)\int_y^{\infty} d\xi\, \frac{1}{2}\mathrm{erfc}(\xi) \\ &+ s(e^{-b} - 1)\int_{-y}^{\infty} d\xi\, \frac{1}{2}\mathrm{erfc}(\xi). \end{aligned} \tag{20}$$

Dilute limit. The limit of small ρ_a and ρ_b corresponds to very few particles compared to the space available. Intuitively,

the dilute limit corresponds to point particles with a noncrossing condition where exact results are available [1,2,20]. We confirm this intuition using a systematic perturbation solution of the general hydrodynamic theory in the low-density limit.

The analysis is similar to that in the dense limit, and we present only the important steps. For simplicity, we shall use similar notations used in the dense limit, but their meaning here will be restricted to the dilute limit unless mentioned otherwise. In the dilute limit, the diffusivity $D(\rho) \simeq D(0)$ and the mobility $\sigma(\rho) \simeq \rho\sigma'(0)$. (The vanishing mobility is by similar reasoning as discussed in the dense limit.) Using an expansion of the least-action paths, $q = q_1 + q_2 + \dots$ a nd $p = p_0 + p_1 + p_2 + \dots$ (the subscript denotes the order in density) in Eq. (5) gives the equation followed by the leading nonvanishing terms p_0 and q_1 which are similar in form with Eq. (10), except for the difference that the terms are for the dilute limit, namely $\alpha = \sigma'(0)/2D(0)$ and $D(1)$ is replaced by $D(0)$. Their general solution is similar to (11b).

A crucial difference with the dense limit comes in the expansion $X_T[q] \equiv Y = Y_0 + Y_1 + \cdots$ in Eq. (2), where Y_0 is nonvanishing and given by the single-file constraint $\int_0^{Y_0} dx\, q_1(x,T) = \int_0^{\infty} dx(q_1(x,T) - q_1(x,0))$. Intuitively, this means that in the dilute limit the tracer can move (in contrast to the dense limit where Y_0 vanishes due to full packing). In fact, by dimensional argument, at low density, the tracer position is expected to scale with the interparticle separation, and thereby inversely with density. This means the CGF in the dilute limit is expected to follow a scaling $\mu(\lambda) \simeq \rho\, h(\lambda/\rho)$. In our perturbation theory, we take this into account by considering λ of the order of the density.

(a) Quenched case. In the dense limit, the boundary condition (8) gives a condition for the leading order $q_1(x,0) = \rho_a\Theta(-x) + \rho_b\Theta(x)$, and $p_0(x,T) = B\,\Theta(x - Y_0)$, where $B = \lambda/q_1(Y_0,T)$.

Similarly, expanding the minimal action (9) for the quenched case, and using the equation for p_0 and q_1 with their boundary conditions, we get [40] the leading order term of the CGF in the dilute limit

$$\mu_{\mathcal{Q}}(\lambda) \simeq \lambda\, Y_0 - \int_{-\infty}^{\infty} dx\, q_1(x,T)p_0(x,T) + \int_{-\infty}^{\infty} dx\, q_1(x,0)p_0(x,0), \tag{21}$$

where Y_0 for the quenched case follows the single-file constraint $\int_{Y_0}^{\infty} dx\,(q_1(x,T) - \rho_b) = Y_0\rho_b$.

The expression (21) requires the solution for $q_1(x,t)$ and $p_0(x,t)$, which is straightforward to get from the general solution (11) by treating B as a parameter in the boundary condition. The solution shows that $q_1(x,T)$ has a jump discontinuity at $x = Y_0$ and therefore B can not be determined self-consistently from its definition. It needs to be determined by further optimizing $\mu_{\mathcal{Q}}$ with respect to B [2]. Using the explicit solution for $q_1(x,t)$ and $p_0(x,t)$ in (21) we get [40] a parametric solution of the CGF in the dense limit

$$\mu_{\mathcal{Q}}(\lambda) \simeq \frac{\sqrt{4D(0)T}}{\alpha}\,\{\alpha\lambda y + R_{\mathcal{Q}}(y,b|\rho_a,\rho_b)\} \tag{22a}$$

with (17b), where y and b are determined from

$$\frac{\partial R_{\mathcal{Q}}}{\partial b} = 0 \quad \text{and} \quad \frac{\partial R_{\mathcal{Q}}}{\partial y} = -\alpha\lambda. \tag{22b}$$

The two relations in (22b) came respectively from the single-file condition for Y_0 and the additional optimization condition $d\mu_{\mathcal{Q}}/dB = 0$.

(b) Annealed case. In the dilute limit, the boundary condition (7) gives

$$p_0(x,0) = B\Theta(x) + \frac{1}{\alpha}\ln\frac{q_1(x,0)}{\bar{\rho}(x)} \tag{23}$$

and $p_0(x,T) = B\Theta(x - Y_0)$, where $B = \lambda/q_1(Y_0,T)$.

Similar to the quenched setting, solutions for $q_1(x,t)$ and $p_0(x,t)$ are determined by treating B as a parameter which is to be determined from an optimization with respect to B.

To the leading order in the dilute limit, the minimal action in Eq. (9) for the annealed case gives the CGF

$$\mu_{\mathcal{A}}(\lambda) \simeq \lambda\, Y_0 + \frac{1}{\alpha}\int_{-\infty}^{\infty} dx\,(q_1(x,0) - \bar{\rho}(x)), \tag{24}$$

where we used a similar identity (16) for the dilute limit, the boundary condition for $p_0(x,T)$, and the single-file constraint $\int_{Y_0}^{\infty} dx\, q_1(x,T) = \int_0^{\infty} dx\, q_1(x,0)$ that is due to (2) in the dilute limit. The single-file condition gives Y_0 in terms of B which is further determined from the optimization condition $d\mu_{\mathcal{A}}/dB = 0$.

Incorporating the solution for $q_1(x,t)$ in (24) and the additional conditions for Y_0 and B, we obtain [40] an expression for the annealed CGF in the dilute limit that is almost identical in form to (22), except the $R_{\mathcal{Q}}$ replaced by $R_{\mathcal{A}}$ defined in (20).

Large deviations. Our primary results are the explicit expression for the CGF in two limiting densities for two different initial states. For the quenched case, the dense limit result is in (17) and the dilute limit result is in (22). Their result for the annealed case are similar in form with $R_{\mathcal{Q}}$ replaced by $R_{\mathcal{A}}$ defined in (20). These results are equivalent of the large time asymptotic of the probability of tracer position

$$P\left(\frac{X_T}{\sqrt{4D_0T}} = y\right) \sim \exp\left[-\frac{\sqrt{4D_0T}}{|\alpha|}\,\phi(y)\right], \tag{25}$$

where $\phi(y)$ is the large deviation function (LDF) and D_0 is the leading diffusivity in the two density limits; α defined earlier in the two limits relates to the isothermal compressibility K_T by $\alpha = \rho K_T$ in the dilute limit, and $\alpha = -K_T/(1-\rho)$ in the dense limit [40]. The LDF relates to the CGF by a Legendre transformation, and using the derived expression for the latter it is straightforward to obtain the following results: In the dense limit,

$$\phi_{\mathcal{Q}(\mathcal{A})}(y) \simeq -by - R_{\mathcal{Q}(\mathcal{A})}(0,b|1-\rho_a,1-\rho_b), \tag{26}$$

and in the dilute limit,

$$\phi_{\mathcal{Q}(\mathcal{A})}(y) \simeq -R_{\mathcal{Q}(\mathcal{A})}(y,b|\rho_a,\rho_b), \tag{27}$$

where for each case the parameter b is determined by an optimization condition $\partial\phi/\partial b = 0$. Similarity of the closed-form-expression for the different limits is encouraging for solutions at arbitrary density.

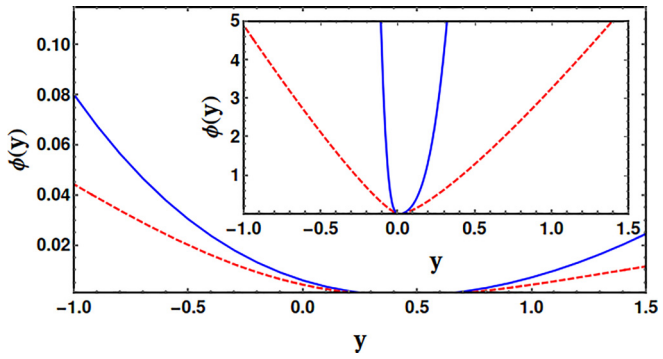

FIG. 2. The large deviation function $\phi(y)$ in (27) for the step initial density with $\rho_a = 0.05$ and $\rho_b = 0.01$ that corresponds to the dilute limit. The blue solid line denotes the quenched case and the red dashed line denotes the annealed case. The inset shows the corresponding results (26) for the dense limit with $\rho_a = 0.99$ and $\rho_b = 0.95$.

Note that the LDF in (25) is independent of specific details of model systems which are in the parameters D_0 and α. The results for $\phi(y)$ in Eq. (26) match with the results [22,23] in the dense limit of the symmetric exclusion process for which $D(\rho) = 1$ and $\sigma = 2\rho(1-\rho)$. Results in Eqs. (27) agree with the results [2,3] for hard-core Brownian point particles.

In the annealed case, expression for LDF can be further simplified to an explicit formula. For the dilute limit we get

$$\phi_A(y) = (\sqrt{\rho_a h(y)} - \sqrt{\rho_b h(-y)})^2 \tag{28}$$

with $h(y) = \frac{1}{2}\int_y^\infty \mathrm{erfc}(x)dx$. (See [40] for a similar formula in the dense limit.)

A comparative plot of the LDF for different cases is shown in Fig. 2 for step initial profiles with $\rho_a > \rho_b$. The step initial state not only drifts the mean position of the tracer, but it also makes fluctuations asymmetric around the mean as seen in the asymmetry of $\phi(y)$. Note that annealed LDF is wider than quenched LDF, which indicates a larger fluctuation for the former case. Similarly, the narrower LDF for the dense limit (inset of Fig. 2) compared to the dilute limit reflects that the tracer is less mobile in the former limit.

Concluding Remarks— We presented analytical results for the long-time statistics of the tracer position in a general single-file diffusion. Our results complement similar recent results [1,3,22,23] for specific model systems obtained using a solution of microscopic dynamics. Besides cumulants, the least action path $q(x,t)$ in our analysis gives how the density profile of surrounding particles evolves leading to a tracer position X_T.

Our analysis presented here is a perturbation solution of the general theory reported earlier in [2]. The theory is based on a hydrodynamic formulation that, although less rigorous than a microscopic solution, gives the correct result for all cumulants at large times and it is applicable for a wider class of systems. However, our perturbation approach relies on the analyticity of the transport coefficients around the two limits, and it would fail for systems like the random average process [41]. For limits where transport coefficients are singular, the weak-noise-theory of MFT is itself questionable.

In our perturbation approach, higher order terms could be systematically solved and that would give improved results for a wider range of density. It would be interesting to compare our general results for rare fluctuations in computer simulation of single-file with different inter-particle interactions. A particularly interesting case is when the tracer is confined in an external potential [23,42,43]. Theoretically, most challenging would be to extend the hydrodynamic approach for biased dynamics, when only the tracer is driven or when all particles are driven [22,23,38,44–47].

Acknowledgments. We acknowledge support of the Department of Atomic Energy, Government of India, under Project Identification No. RTI-4002.

[1] N. Leibovich and E. Barkai, Phys. Rev. E **88**, 032107 (2013).
[2] P. L. Krapivsky, K. Mallick, and T. Sadhu, Phys. Rev. Lett. **113**, 078101 (2014); J. Stat. Phys. **160**, 885 (2015).
[3] T. Sadhu and B. Derrida, J. Stat. Mech.: Theory Exp. (2015) P09008.
[4] P. L. Krapivsky, K. Mallick, and T. Sadhu, J. Stat. Mech.: Theory Exp. (2015) P09007.
[5] A. L. Hodgkin and R. Keynes, The Journal of Physiology **128**, 61 (1955).
[6] J. Kärger and D. M. Ruthven, *Diffusion in Zeolites and Other Microporous Solids* (Wiley, New York, 1992)
[7] T. Chou and D. Lohse, Phys. Rev. Lett. **82**, 3552 (1999).
[8] A. Das, S. Jayanthi, H. S. M. V. Deepak, K. V. Ramanathan, A. Kumar, C. Dasgupta, and A. K. Sood, ACS Nano **4**, 1687 (2010).
[9] G.-W. Li, O. G. Berg, and J. Elf, Nature (London) **5**, 294 (2009).
[10] P. M. Richards, Phys. Rev. B **16**, 1393 (1977).
[11] T. E. Harris, J. Appl. Probab. **2**, 323 (1965).
[12] V. Kukla, J. Kornatowski, D. Demuth, I. Girnus, H. Pfeifer, L. V. Rees, S. Schunk, K. K. Unger, and J. Kärger, Science **272**, 702 (1996).
[13] Q.-H. Wei, C. Bechinger, and P. Leiderer, Science **287**, 625 (2000).
[14] C. Lutz, M. Kollmann, and C. Bechinger, Phys. Rev. Lett. **93**, 026001 (2004).
[15] B. Lin, M. Meron, B. Cui, S. A. Rice, and H. Diamant, Phys. Rev. Lett. **94**, 216001 (2005).
[16] C. Rödenbeck, J. Kärger, and K. Hahn, Phys. Rev. E **57**, 4382 (1998).
[17] M. Kollmann, Phys. Rev. Lett. **90**, 180602 (2003).
[18] L. Lizana and T. Ambjörnsson, Phys. Rev. Lett. **100**, 200601 (2008).
[19] R. Arratia, The Annals of Probability **11**, 362 (1983).
[20] T. Imamura, K. Mallick, and T. Sasamoto, Phys. Rev. Lett. **118**, 160601 (2017).
[21] A. Grabsch, A. Poncet, P. Rizkallah, P. Illien, and O. Bénichou, Sci. Adv. **8**, eabm5043 (2022).
[22] A. Poncet, O. Bénichou, and P. Illien, Phys. Rev. E **103**, L040103 (2021).
[23] P. Illien, O. Bénichou, C. Mejía-Monasterio, G. Oshanin, and R. Voituriez, Phys. Rev. Lett. **111**, 038102 (2013).

[24] L. Bertini, A. De Sole, D. Gabrielli, G. Jona-Lasinio, and C. Landim, Phys. Rev. Lett. **87**, 040601 (2001).
[25] L. Bertini, A. De Sole, D. Gabrielli, G. Jona-Lasinio, and C. Landim, J. Stat. Phys. **107**, 635 (2002).
[26] L. Bertini, A. De Sole, D. Gabrielli, G. Jona-Lasinio, and C. Landim, Phys. Rev. Lett. **94**, 030601 (2005).
[27] L. Bertini, A. De Sole, D. Gabrielli, G. Jona-Lasinio, and C. Landim, J. Stat. Phys. **135**, 857 (2009).
[28] L. Bertini, A. De Sole, D. Gabrielli, G. Jona-Lasinio, and C. Landim, Rev. Mod. Phys. **87**, 593 (2015).
[29] L. Onsager and S. Machlup, Phys. Rev. **91**, 1505 (1953).
[30] A. Krajenbrink and P. Le Doussal, Phys. Rev. Lett. **127**, 064101 (2021).
[31] E. Bettelheim, N. R. Smith, and B. Meerson, J. Stat. Mech.: Theory Exp. (2022) 093103.
[32] K. Mallick, H. Moriya, and T. Sasamoto, Phys. Rev. Lett. **129**, 040601 (2022).
[33] T. Bodineau and B. Derrida, C. R. Phys. **8**, 540 (2007).
[34] A. Poncet, A. Grabsch, P. Illien, and O. Bénichou, Phys. Rev. Lett. **127**, 220601 (2021).
[35] B. Derrida, J. Stat. Mech.: Theory Exp. (2007) P07023.
[36] P. C. Martin, E. Siggia, and H. Rose, Phys. Rev. A **8**, 423 (1973); C. De Dominicis and L. Peliti, Phys. Rev. B **18**, 353 (1978).
[37] M. Mezard, G. Parisi, and M. Virasoro, *Spin Glass Theory and Beyond* (World Scientific, 1986).
[38] T. Imamura and T. Sasamoto, J. Stat. Phys. **128**, 799 (2007).
[39] B. Derrida and A. Gerschenfeld, J. Stat. Phys. **137**, 978 (2009).
[40] See Supplemental Material at http://link.aps.org/supplemental/10.1103/PhysRevE.107.L012101 for important steps to derive the large deviation functions in both limits and its relation with bulk compressibility.
[41] A. Kundu and J. Cividini, Europhys. Lett. **115**, 54003 (2016).
[42] S. Burlatsky, G. Oshanin, A. Mogutov, and M. Moreau, Phys. Lett. A **166**, 230 (1992).
[43] S. F. Burlatsky, G. Oshanin, M. Moreau, and W. P. Reinhardt, Phys. Rev. E **54**, 3165 (1996).
[44] R. Rajesh and S. N. Majumdar, Phys. Rev. E **64**, 036103 (2001).
[45] E. Barkai and R. Silbey, Phys. Rev. Lett. **102**, 050602 (2009).
[46] S. N. Majumdar and M. Barma, Phys. Rev. B **44**, 5306 (1991).
[47] A. De Masi and P. A. Ferrari, J. Stat. Phys. **38**, 603 (1985).